Model-Based Quantification of Impact of Genetic Polymorphisms and Co-Medications on Pharmacokinetics of Tamoxifen and Six Metabolites in Breast Cancer

Alicja Puszkiel[1], Cécile Arellano[1], Christelle Vachoux[1], Alexandre Evrard[2,3], Valérie Le Morvan[4,5], Jean-Christophe Boyer[2], Jacques Robert[4,5], Caroline Delmas[1,6], Florence Dalenc[1,6], Marc Debled[5], Laurence Venat-Bouvet[7], William Jacot[8], Nadine Dohollou[9], Chantal Bernard-Marty[10], Hortense Laharie-Mineur[11], Thomas Filleron[6], Henri Roché[6], Etienne Chatelut[1,6], Fabienne Thomas[1,6,†] and Melanie White-Koning[1,*,†]

Variations in clinical response to tamoxifen (TAM) may be related to polymorphic cytochromes P450 (CYPs) involved in forming its active metabolite endoxifen (ENDO). We developed a population pharmacokinetic (PopPK) model for tamoxifen and six metabolites to determine clinically relevant factors of ENDO exposure. Concentration-time data for TAM and 6 metabolites come from a prospective, multicenter, 3-year follow-up study of adjuvant TAM (20 mg/day) in patients with breast cancer, with plasma samples drawn every 6 months, and genotypes for 63 genetic polymorphisms (PHACS study, NCT01127295). Concentration data for TAM and 6 metabolites from 928 patients (n = 27,433 concentrations) were analyzed simultaneously with a 7-compartment PopPK model. CYP2D6 phenotype (poor metabolizer (PM), intermediate metabolizer (IM), normal metabolizer (NM), and ultra-rapid metabolizer (UM)), *CYP3A4*22*, *CYP2C19*2*, and *CYP2B6*6* genotypes, concomitant CYP2D6 inhibitors, age, and body weight had a significant impact on TAM metabolism. Formation of ENDO from N-desmethyltamoxifen was decreased by 84% (relative standard error (RSE) = 14%) in PM patients and by 47% (RSE = 9%) in IM patients and increased in UM patients by 27% (RSE = 12%) compared with NM patients. Dose-adjustment simulations support an increase from 20 mg/day to 40 and 80 mg/day in IM patients and PM patients, respectively, to reach ENDO levels similar to those in NM patients. However, when considering Antiestrogenic Activity Score (AAS), a dose increase to 60 mg/day in PM patients seems sufficient. This PopPK model can be used as a tool to predict ENDO levels or AAS according to the patient's CYP2D6 phenotype for TAM dose adaptation.

Study Highlights

WHAT IS THE CURRENT KNOWLEDGE ON THE TOPIC?

☑ Plasma concentrations of endoxifen, the main active metabolite of tamoxifen (TAM), show high interindividual variability due to genetic and demographic factors as well as concomitant treatments.

WHAT QUESTION DID THE STUDY ADDRESS?

☑ What is the quantitative impact of genetic polymorphisms and co-medications on pharmacokinetic (PK) parameters of TAM and its metabolites?

WHAT DOES THIS STUDY ADD TO OUR KNOWLEDGE?

☑ Using a population PK analysis for TAM and six major metabolites with prospective 3-year follow-up on 928 patients receiving adjuvant TAM, this study shows that CYP2D6 phenotype, *CYP3A4*22*, *CYP2C19*2*, and *CYP2B6*6* genotype, concomitant CYP2D6 inhibitors, age, and body weight had a significant impact on TAM metabolism.

HOW MIGHT THIS CHANGE CLINICAL PHARMACOLOGY OR TRANSLATIONAL SCIENCE?

☑ Simulation results derived from this PK model support a dose increase in patients with impaired CYP2D6 metabolism, so that they can reach a median ENDO concentration or antiestrogenic activity score similar to that observed in normal metabolizer patients.

[1]Cancer Research Center of Toulouse (CRCT), Inserm U1037, Université Paul Sabatier, Toulouse, France; [2]Laboratoire de Biochimie et Biologie Moléculaire, Centre Hospitalier Universitaire Nîmes-Carémeau, Nîmes, France; [3]IRCM, Inserm, Université de Montpellier, ICM, Montpellier, France; [4]Inserm U1218, Université de Bordeaux, Bordeaux, France; [5]Institut Bergonié, Bordeaux, France; [6]Institut Claudius Regaud, Institut Universitaire du Cancer de Toulouse – Oncopole, Toulouse, France; [7]Centre Hospitalier Universitaire Dupuytren, Limoges, France; [8]Institut du Cancer de Montpellier, Montpellier, France; [9]Polyclinique Bordeaux Nord Aquitaine, Bordeaux, France; [10]Clinique Pasteur – ONCORAD, Toulouse, France; [11]Clinique Tivoli-Ducos, Bordeaux, France. *Correspondence: Melanie White-Koning (melanie.white-koning@univ-tlse3.fr)

[†]These authors shared senior authorship of this study.

Received July 21, 2020; accepted October 4, 2020. doi:10.1002/cpt.2077

Tamoxifen (TAM), a selective estrogen receptor modulator, has been the cornerstone of estrogen receptor-positive breast cancer treatment for over 40 years. TAM undergoes a complex metabolism with over 20 identified metabolites[1,2] of which (Z)-endoxifen (ENDO) and (Z)-4-hydroxytamoxifen (4-OHTAM) have ~ 30–100 fold-higher activity than the parent compound.[3,4] The metabolism of TAM is mediated by cytochrome P450 (CYP) family isoenzymes.[1,2] CYP3A4/5 is the main enzyme involved in the formation of TAM major metabolite N-desmethyltamoxifen (NDT) and CYP2D6 is the only enzyme responsible for its further conversion to ENDO. The formation of 4-OHTAM from TAM is mediated mainly by CYP2D6, although other isoenzymes (CYP2C9, CYP2C19, and CYP3A4) are involved. The conversion of 4-OHTAM to ENDO is mediated mainly by CYP3A4/5. Genetic polymorphisms, co-medications, and other factors affecting CYP isoenzymes activity impact plasma concentrations of active metabolites with possible consequences for therapeutic outcome. Extensive research has been carried out to understand the high interindividual variability (IIV) of TAM efficacy and toxicity, with conflicting results concerning the relationship between *CYP2D6* genotype and TAM efficacy,[5–7] and the association between plasma ENDO concentrations and clinical outcomes.[8–11] In particular, the recent CYPTAM study showed no association between plasma concentrations of ENDO and relapse-free survival in 667 patients with early-stage breast cancer.[11,12] However, as pointed out by several experts, the study design was insufficient to answer the question of an association between TAM metabolism and efficacy[13,14] and this study did not investigate intermediate metabolites.

To date, three population pharmacokinetic (PK) models describing disposition of both TAM and ENDO have been reported. In two of them,[15,16] TAM was directly converted to ENDO without accounting for intermediate metabolites, which does not allow for an accurate quantification of the impact of genetic polymorphisms on TAM metabolism. In the third model,[17] CYP2D6 genotyping was only performed for **3*, **4*, **5*, and **6* variant alleles.

Hence, our aim was to (i) develop a population PK model describing steady-state concentrations of TAM and its six major metabolites in a large, longitudinal, prospective study of patients with breast cancer treated with TAM 20 mg/day in an adjuvant setting, and (ii) quantify the impact of genetic polymorphisms, comedications, and demographic characteristics on the pharmacokinetics (PKs) of TAM and its metabolites. The final PK model was subsequently used to evaluate the alternative dosing regimens necessary to reach a target exposure to ENDO and other active metabolites in patients with impaired CYP2D6 activity.

METHODS

Study population

Data come from a prospective, multicenter, 3-year follow-up study aiming to investigate the relationship among PK, pharmacogenetics, and toxicity of TAM and aromatase inhibitors in 1977 patients with adjuvant breast cancer (PHACS; ClinicalTrials.gov NCT01127295).[18] When TAM was selected as the recommended drug, 879 patients started treatment at 20 mg/day and were followed up every 6 months over 3 years. Moreover, some patients underwent a switch from aromatase inhibitors to TAM during the 3-year period. Current analyses were performed on 928 patients taking TAM at some point over the course of their treatment for whom PK data was available. All patients provided written informed consent as per the revised Declaration of Helsinki and French regulations.

Data collection

Blood samples for PK analysis were collected in lithium heparinized Vacutainer tubes at inclusion and 24 hours postdose every 6 months during the 3-year follow-up. In addition, comedication data at the time of PK sampling and adherence data during the month preceding the visit were reported by the clinician based on an interview with the patient. Samples were centrifuged at 1,400 × *g* at ambient temperature and plasma was stored at −20°C until analysis. Plasma concentrations of TAM, NDT, tamoxifen N-oxide (NOX-TAM), 4-OHTAM, (Z)-4′-hydroxytamoxifen (4′-OHTAM), ENDO and (Z′)-endoxifen (Z′-ENDO) were quantified by a validated ultraperformance liquid chromatography-tandem mass spectrometry method.[19] The lower limit of quantification (LLOQ) was 5 ng/mL for TAM, NDT, and NOX-TAM and 0.5 ng/mL for 4-OHTAM, 4′-OHTAM, ENDO, and Z′-ENDO. Blood samples for genotyping were collected at study inclusion. The analysis of 63 selected single nucleotide polymorphisms in genes of interest was described elsewhere.[18] Based on the presence of respective *CYP2D6* alleles (**4*, **6*, **7*, **9*, **10*, **17*, and **41*) and the number of gene copies (**5* or duplication), patients were assigned a CYP2D6 diplotype and activity score (AS). Finally, patients were classified into poor metabolizer (PM), intermediate metabolizer (IM), normal metabolizer (NM) or ultrarapid metabolizer (UM) CYP2D6 phenotype according to Caudle *et al.*,[20] as described in **Supplementary Material S1**.

Population pharmacokinetic analysis

The development of a joint parent-metabolite model was performed in a stepwise manner using NONMEM software. First, a one-compartment model with first-order absorption and elimination was used to fit concentration-time data of the parent compound (TAM). Once the TAM model was developed, NDT, 4-OHTAM, and ENDO data were included sequentially in the model allowing for development of a central model describing ENDO formation (**Figure 1**). The volumes of distribution of the metabolites were not identifiable and were not available from literature. Therefore, in this study, the volumes of distribution of all the metabolites were fixed to V_{TAM}, as is common practice.[21] The TAM absorption rate constant k_a was fixed in the models including metabolites. In the following step, the Z′-ENDO metabolite formed from NDT was included. Intermediate models for 4′-OHTAM and NOX-TAM were developed, including one compartment for TAM and one for the other metabolite. The parameter estimates from these intermediate models were used as initial estimates in the full metabolite model.

IIV was included on PK parameters assuming a log-normal distribution. The inclusion of interoccasion variability on PK parameters was tested. The residual variability was estimated separately for each compound according to a proportional error model. Covariates were included in the model according to standard methodology described in more detail in **Supplementary Material S1**.

To evaluate the simulation performance of the model, steady-state trough concentrations ($C_{ss,trough}$) of ENDO were simulated according to CYP2D6 diplotype (n = 1,000 for each diplotype), using our final model and the model recently reported by Mueller-Schoell *et al.*,[16] and were compared with the steady-state values reported by Teft *et al.*[22]

Model-based simulations were performed to evaluate the impact of CYP2D6 phenotype and all the significant covariates on plasma ENDO exposure. Plasma ENDO $C_{ss,trough}$ were simulated according to CYP2D6 phenotype and categorical covariates (n = 1,000 for each combination of CYP2D6 phenotype + categorical covariate) using the estimates of the final model.

Dose-adjustment simulations were performed in patients at increased risk of subtherapeutic ENDO $C_{ss,trough}$, with alternative doses selected for simulations in CYP2D6 IM patients (40 mg/day) and PM patients (40, 60, and 80 mg/day, n = 1,000 for each dose). As recently

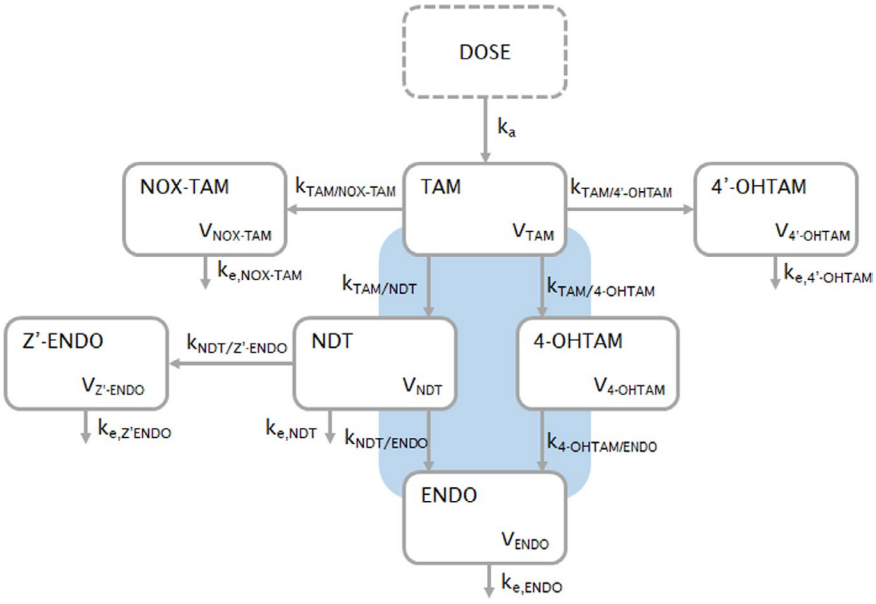

Figure 1 Schematic representation of the structural model for TAM and its six major metabolites. The shaded area represents the major metabolic pathways leading to active metabolite ENDO. 4′-OHTAM, 4′-hydroxytamoxifen; 4-OHTAM, 4-hydroxytamoxifen; ENDO, endoxifen; k, conversion rate constant; k_a, absorption rate constant; k_e, elimination rate constant; NDT, N-desmethyltamoxifen; NOX-TAM, tamoxifen N-oxide; TAM, tamoxifen; V, volume of distribution; Z′-ENDO, Z′-endoxifen. [Colour figure can be viewed at wileyonlinelibrary.com]

used by Mueller-Schoell *et al*.,[16] the previously reported ENDO $C_{ss,trough}$ of 16 nM, associated with a 26% reduction of breast cancer recurrence in an adjuvant setting,[8] was used as the therapeutic target threshold. However, as this threshold has not been validated in other recent prospective studies,[11] the median observed ENDO $C_{ss,trough}$ in patients with CYP2D6 NM phenotype, *CYP3A4*22*, *CYP2C19*2*, and *CYP2B6*6* noncarriers and no concomitant intake of CYP2D6 inhibitors was used as an alternative reference value in the simulations (40 nM, $n = 166$). In addition, the Antiestrogenic Activity Score (AAS) suggested by de Vries Schultink *et al*. was also considered as a surrogate for clinical response.[23] The AAS takes into account plasma concentrations of TAM, NDT, 4-OHTAM, and ENDO and their respective anti-estrogenic activity. In the same manner as for ENDO $C_{ss,trough}$, the therapeutic AAS cutoff value of 1,798 proposed by de Vries Schultink *et al*. and the median AAS of 3,753 (in patients with CYP2D6 NM phenotype, *CYP3A4*22*, *CYP2C19*2*, and *CYP2B6*6* wild-type genotype, and no concomitant intake of CYP2D6 inhibitors, $n = 166$) were selected as threshold and reference values for the simulations.

Finally, additional dose-adjustment simulations were performed using the model, including CYP2D6 diplotype on $k_{NDT/ENDO}$ with alternative doses of 40, 60, and 80 mg/day for PM/PM, IM/PM, IM/IM, NM/PM, and NM/IM patients ($n = 1{,}000$ for each dose).

RESULTS

Patient characteristics and data

The genetic and demographic characteristics of 928 patients included in the analysis are summarized in **Table 1**. At each time point, if TAM and all six metabolite concentrations were below the LLOQ, the samples were excluded ($n = 71$, representing 1.8% of the dataset), leaving a total of 3,919 time points (27,433 plasma concentrations) in the analysis. Of those, 464 concentrations (1.7%) were below the LLOQ and were included in the analysis with a value set to LLOQ/2. The median (interquartile range) of the sampling time was 24.2 hours (19.8–25.3 hours) and the number of samples taken more than 48 hours after the last dose corresponded to 2% of the entire dataset. Two hundred sixty-one (6.6%) plasma concentrations with missing time after dose were included in the analysis and were considered as taken 24 hours after dose. Concomitant use of CYP2D6 inhibitors was recorded at 253 follow-up visits corresponding to 126 patients. If at the same visit, a concomitant intake of two or more CYP2D6 inhibitors was recorded, the sum of the inhibitory potency of each drug (weak = 1, moderate = 2, and potent = 3) was considered.

Population pharmacokinetic analysis

Model development. The concentration-time data of TAM and six metabolites were described simultaneously by a seven-compartment model (**Figure 1**). Because of the sparse study design, estimation of all parameters was not possible (high relative standard error) therefore, the elimination rate constants of Z′-ENDO, 4′-OHTAM, and NOX-TAM in the final model were fixed to the values estimated in intermediate models. The parameters on which IIV was included can be found in **Table 2**. The data did not support estimation of IIV on $k_{NDT/Z'ENDO}$, $k_{4\text{-}OHTAM/ENDO}$, and $k_{e,ENDO}$, which was therefore fixed to 0. The η-shrinkage was small (< 14%) except for $k_{TAM/4'\text{-}OHTAM}$ (29%). Interoccasion variability was tested on several parameters but resulted in significantly increased η-shrinkage (> 20%) and hence was not retained in the model. The model fit the data well as shown by acceptable proportional residual error values (**Table 2**) associated with low ε-shrinkage (< 8.4%).

Covariate analysis. Covariate relationships were investigated for $k_{TAM/NDT}$, $k_{TAM/4\text{-}OHTAM}$, $k_{TAM/NOX\text{-}TAM}$, $k_{NDT/ENDO}$, and $k_{e,NDT}$. The results of the univariate covariate inclusion in the base model are presented in **Table S1**. CYP2D6 phenotype,

Table 1 Patients' characteristics (*n* = 928)

Characteristic	Median [range] or number (%)
Age at inclusion, years	48 [25–84]
Body weight, kg	64 [40–131]
CYP2D6 phenotype	
Ultra-rapid metabolizer	32 (3.7)
Normal metabolizer	730 (83.3)
Intermediate metabolizer	75 (8.6)
Poor metabolizer	39 (4.4)
Missing	52
*CYP3A4*22* genotype	
Wild-type (**1/*1*)	836 (91.2)
Heterozygous mutant (**1/*22*)	78 (8.5)
Homozygous mutant (**22/*22*)	3 (0.3)
Missing	11
*CYP3A4*1B* genotype	
Wild-type (**1/*1*)	857 (93.3)
Heterozygous mutant (**1/*1B*)	58 (6.3)
Homozygous mutant (**1B/*1B*)	4 (0.4)
Missing	9
*CYP3A5*3* genotype	
Wild-type (**1/*1*)	6 (0.7)
Heterozygous mutant (**1/*3*)	122 (13.3)
Homozygous mutant (**3/*3*)	786 (86.0)
Missing	14
*CYP2C19*2* genotype	
Wild-type (**1/*1*)	654 (71.2)
Heterozygous mutant (**1/*2*)	244 (26.6)
Homozygous mutant (**2/*2*)	20 (2.2)
Missing	10
*CYP2C19*17* genotype	
Wild-type (**1/*1*)	568 (62.1)
Heterozygous mutant (**1/*17*)	308 (33.7)
Homozygous mutant (**17/*17*)	38 (4.2)
Missing	14
*CYP2B6*6* genotype	
Wild-type (**1/*1*)	497 (55.2)
Heterozygous mutant (**1/*6*)	347 (38.6)
Homozygous mutant (**6/*6*)	56 (6.2)
Missing	28
Comedications	**Number of occasions**
CYP2D6 inhibitors	
Weak[a]	135
Moderate[b]	44
Potent[c]	74
CYP3A4 inhibitors	
Weak[d]	109
Moderate[e]	41
Potent[f]	15

[a]Weak CYP2D6 inhibitors: amiodarone, celecoxib, escitalopram, and sertraline. [b]Moderate CYP2D6 inhibitors: citalopram, diphenhydramine, and duloxetine. [c]Potent CYP2D6 inhibitors: clomipramine, flecainide, fluoxetine, fusidic acid, imatinib, paroxetine, propafenon, and terbinafine. [d]Weak CYP3A4 inhibitors: esomeprazole and omeprazole. [e]Moderate CYP3A4 inhibitors: ciprofloxacin, diltiazem, fluconazole, fluoxetine, imatinib, and verapamil. [f]Potent CYP3A4 inhibitors: clarithromycin, amiodarone, fusidic acid, ketoconazole, and miconazole.

*CYP3A4*22*, *CYP2C19*2*, and *CYP2B6*6* genotypes, concomitant CYP2D6 inhibitors, age, and body weight (BW) were retained in the final multivariate model (**Table 2**). The details of the covariate analysis are presented below.

Estimation of a separate $k_{NDT/ENDO}$ for each CYP2D6 phenotype resulted in a significant decrease in objective function value (OFV; ΔOFV = −430 points, $P < 0.00001$). The mean $k_{NDT/ENDO}$ was 84% (95% confidence interval 79; 88) and 47% (95% confidence interval 38; 57) lower in PM and IM patients, respectively, and 27% (−2; 56) higher in UM patients, compared with NM patients.

An alternative analysis was performed using CYP2D6 diplotype classification (7 categories: PM/PM, IM/PM, IM/IM, NM/PM, NM/IM, NM/NM (reference category), and NM/NM/IM + UM/UM) instead of phenotype in the base model. The inclusion of CYP2D6 diplotype on $k_{NDT/ENDO}$ resulted in a significant improvement of the model fit (ΔOFV = −611 points, $P < 0.00001$) and showed a gradual decrease of the estimates of this parameter with a decrease in CYP2D6 activity. Concerning $k_{TAM/4\text{-}OHTAM}$, the inclusion of CYP2D6 diplotype classification resulted in very close estimates for the different categories, therefore, we decided to use the phenotype classification for this parameter. CYP2D6 phenotype classification was retained in the final model for a more straightforward clinical interpretation but the results of the additional analysis with CYP2D6 diplotypes (included in the final model on $k_{NDT/ENDO}$) are presented in **Table 2**.

Weak/moderate and potent CYP2D6 inhibitors were associated with a 32% (23; 41) and 57% (51; 62) decrease in $k_{NDT/ENDO}$ in both NM and UM patients but had no significant impact on $k_{NDT/ENDO}$ in PM nor in IM patients. In the final model, 37% of the IIV on $k_{NDT/ENDO}$ was explained by both CYP2D6 phenotype and CYP2D6 inhibitors (decrease from 74.8% to 47.4%).

A common effect of CYP2D6 PM and IM phenotypes was estimated on $k_{TAM/4\text{-}OHTAM}$. Both of these phenotypes were associated with a 23% (17; 30) decrease in $k_{TAM/4\text{-}OHTAM}$ compared with NM and UM phenotype. CYP2D6 inhibitors had no statistically significant impact on $k_{TAM/4\text{-}OHTAM}$.

In *CYP3A4*22* carriers, the mean $k_{TAM/NDT}$ and $k_{e,NDT}$ were decreased by 23% (13; 32) and 19% (5; 33) respectively, compared with wild-type patients. Presence of 1 or 2 *CYP2C19*2* allele was associated with a 13% (6; 20) decrease in $k_{TAM/4\text{-}OHTAM}$. Finally, patients with *CYP2B6*6/*6* genotype showed a 23% (13; 34) decrease in $k_{TAM/NOX\text{-}TAM}$ compared with *CYP2B6 *1/*6* and **1/*1* patients.

Age was significantly associated with $k_{TAM/NDT}$, $k_{TAM/4\text{-}OHTAM}$, $k_{TAM/NOX\text{-}TAM}$, and $k_{NDT/ENDO}$ with a decrease of 9%, 15%, 9%, and 13%, respectively, for a 65-year-old patient (95th percentile) compared with a patient with median age (48 years) and the same CYP2D6 phenotype.

A significant association was also found between BW and $k_{e,NDT}$ (9.7% increase in $k_{e,NDT}$ for an increase in BW from 64 kg (median) to 94 kg (95th percentile)).

Model validation. The goodness-of-fit plots of the final model are presented in **Figure S1**. The validation of the final model was

Table 2 Parameter estimates of the final pharmacokinetic model with CYP2D6 status coded as phenotype or as diplotype

	Mean estimate (RSE %) [shrinkage %]		
Parameter (unit)	Final model with CYP2D6 phenotype	Final model with CYP2D6 diplotype	
k_a (h^{-1})	0.90 fixed	0.90 fixed	
V_{TAM} (L)	1,380 (5.4)	1,410 (5.5)	
$k_{TAM/NDT}$ (h^{-1})	5.20×10^{-3} (5.2)	5.12×10^{-3} (5.3)	
Effect of *CYP3A4*22* genotype[a]	0.773 (6.2)	0.772 (6.2)	
Effect of age	−0.298 (20.2)	−0.299 (20.1)	
$k_{TAM/4\text{-}OHTAM}$ (h^{-1})	3.72×10^{-5} (27.2)	3.03×10^{-5} (31.9)	
Effect of CYP2D6 IM or PM phenotype[b]	0.768 (4.4)	0.768 (4.2)	
Effect of CYP2D6 missing phenotype	1.25 (6.8)	1.24 (6.9)	
Effect of *CYP2C19*2* genotype[c]	0.866 (4.1)	0.866 (4.1)	
Effect of age	−0.547 (21.0)	−0.548 (20.6)	
$k_{TAM/4'\text{-}OHTAM}$ (h^{-1})	6.16×10^{-8} (1.6)	6.17×10^{-8} (1.6)	
$k_{TAM/NOX\text{-}TAM}$ (h^{-1})	2.48×10^{-7} (2.3)	2.48×10^{-7} (2.3)	
Effect of *CYP2B6*6/*6* genotype[d]	0.766 (7.2)	0.767 (7.2)	
Effect of age	−0.296 (35.1)	−0.293 (35.5)	
$k_{NDT/ENDO}$			
CYP2D6 UM (h^{-1})	6.87×10^{-4} (11.6)	NM/NM/IM and UM/UM (h^{-1})	7.24×10^{-4} (10.2)
CYP2D6 NM (h^{-1})	5.42×10^{-4} (9.2)	NM/NM (h^{-1})	6.39×10^{-4} (8.8)
		NM/IM (h^{-1})	4.36×10^{-4} (9.3)
CYP2D6 IM (h^{-1})	2.86×10^{-4} (9.2)	NM/PM (h^{-1})	3.61×10^{-4} (8.8)
		IM/IM (h^{-1})	1.93×10^{-4} (15.1)
		IM/PM (h^{-1})	1.68×10^{-4} (9.9)
CYP2D6 PM (h^{-1})	0.88×10^{-4} (14.3)	PM/PM (h^{-1})	0.94×10^{-4} (12.3)
Missing CYP2D6 phenotype (h^{-1})	6.04×10^{-4} (12.2)	Missing diplotype (h^{-1})	6.40×10^{-4} (10.7)
Effect of weak/moderate CYP2D6 inhibitor in NM and UM patients	0.680 (6.9)	0.675 (6.3)	
Effect of potent CYP2D6 inhibitor in NM and UM patients	0.434 (6.3)	0.407 (5.9)	
Effect of age	−0.480 (22.3)	−0.382 (23.6)	
$k_{NDT/Z'\text{-}ENDO}$ (h^{-1})	4.08×10^{-7} (1.0)	4.08×10^{-7} (1.0)	
$k_{4\text{-}OHTAM/ENDO}$ (h^{-1})	1.81×10^{-3} (26.5)	1.48×10^{-3} (31.2)	
$k_{e,NDT}$ (h^{-1})	2.46×10^{-3} (7.4)	2.39×10^{-3} (7.5)	
Effect of *CYP3A4*22* genotype[a]	0.812 (8.7)	0.808 (8.8)	
Effect of body weight	0.245 (21.4)	0.243 (21.8)	
$k_{e,ENDO}$ (h^{-1})	7.93×10^{-3} (8.4)	8.15×10^{-3} (8.1)	
$k_{e,4'\text{-}OHTAM}$ (h^{-1})	2.01×10^{-6} fixed	2.01×10^{-6} fixed	
$k_{e,NOX\text{-}TAM}$ (h^{-1})	1.77×10^{-6} fixed	1.77×10^{-6} fixed	
$k_{e,Z'ENDO}$ (h^{-1})	1.08×10^{-5} fixed	1.08×10^{-5} fixed	
IIV			
$k_{TAM/NDT}$ (% CV)	31.6% (2.9) [6.5]	31.5% (2.9) [6.5]	
$k_{TAM/4\text{-}OHTAM}$ (% CV)	50.6% (3.1) [8.5]	50.6% (3.0) [8.5]	
$k_{TAM/4'\text{-}OHTAM}$ (% CV)	19.6% (4.8) [29]	19.6% (4.8) [29]	
$k_{TAM/NOX\text{-}TAM}$ (% CV)	44.9% (3.2) [14]	44.9% (3.2) [14]	
$k_{NDT/ENDO}$ (% CV)	47.4% (3.4) [12]	39.4% (3.3) [12]	
$k_{e,NDT}$ (% CV)	47.3% (2.8) [4.4]	48.1% (2.8) [4.4]	

(Continues)

Table 2 (Continued)

Parameter (unit)	Mean estimate (RSE %) [shrinkage %]	
	Final model with CYP2D6 phenotype	Final model with CYP2D6 diplotype
Residual variability		
TAM (% CV)	30.9 (1.6) [6.3]	30.9 (1.6) [6.3]
NDT (% CV)	34.4 (2.1) [4.9]	34.4 (2.1) [4.9]
4-OHTAM (% CV)	38.0 (1.8) [8.4]	38.0 (1.8) [8.4]
ENDO (% CV)	40.9 (1.8) [7.3]	41.2 (1.9) [7.3]
Z′-ENDO (% CV)	40.5 (1.5) [3.5]	40.5 (1.5) [3.5]
4′-OHTAM (% CV)	34.9 (1.7) [6.7]	34.9 (1.8) [6.7]
NOX-TAM (% CV)	59.0 (1.9) [6.0]	59.0 (1.9) [6.0]

4′-OHTAM, 4′-hydroxytamoxifen; 4-OHTAM, 4-hydroxytamoxifen; CV, coefficient of variation; ENDO, endoxifen; IIV, interindividual variability; IM, CYP2D6 intermediate metabolizer; k, conversion rate constant; k_a, absorption rate constant; k_e, elimination rate constant; NDT, N-desmethyltamoxifen; NM, CYP2D6 normal metabolizer; NOX-TAM, tamoxifen N-oxide; PM, CYP2D6 poor metabolizer; RSE, relative standard error; TAM, tamoxifen; UM, CYP2D6 ultrarapid metabolizer; V_{TAM}, apparent volume of distribution of TAM; Z′-ENDO, Z′-endoxifen;
[a]Reference: *CYP3A4*22* non-carriers. [b]Reference: CYP2D6 NM and UM. [c]Reference: *CYP2C19*2* non-carriers. [d]Reference: *CYP2B6*1/*6* and *CYP2B6*1/*1*.

based on a visual predictive check (VPC) with 1,000 replicates of the original dataset (**Figure 2**). The VPC indicates that the predictive performance of the model is accurate for all compounds although the concentrations of NOX-TAM are overestimated by the model due to a decrease of its concentrations with time, which could not be accounted for in the model. Because NOX-TAM is not an active TAM metabolite, this was not considered deleterious for the validity of the model-based simulations. Moreover, the final model showed good simulation performance as most of the simulated ENDO concentrations fell within one SD of the mean of the values reported in the study by Teft *et al.*[22] and were comparable to those simulated using the recently published Mueller-Schoell model[16] (data not shown).

Simulations

The impact of CYP2D6 phenotype, *CYP3A4*22*, *CYP2C19*2*, and *CYP2B6*6* genotypes and CYP2D6 inhibitors on plasma ENDO $C_{ss,trough}$ was investigated through simulations. ENDO $C_{ss,trough}$ were simulated for each CYP2D6 phenotype and wild-type genotype for *CYP3A4*22*, *CYP2C19*2*, and *CYP2B6*6* and no concomitant CYP2D6 inhibitors (n = 1,000 for each CYP2D6 phenotype). Then, for each CYP2D6 phenotype, simulations of ENDO concentrations according to the presence of *CYP3A4*22*, *CYP2C19*2* alleles, or *CYP2B6*6/*6* genotype, or concomitant use of a weak/moderate or potent CYP2D6 inhibitor were performed allowing for variation of only one covariate at a time (n = 1,000 for each combination; **Figure 3**). In patients with wild-type *CYP3A4*22*, *CYP2C19*2*, and *CYP2B6*6* and no concomitant inhibitors, the median ENDO $C_{ss,trough}$ were 77% and 38% lower in PM and IM patients, respectively, and 25% higher in UM patients compared with NM. For a given CYP2D6 phenotype, median ENDO $C_{ss,trough}$ was 16–25% higher (depending on CYP2D6 phenotype) in patients homozygous or heterozygous for *CYP3A4*22* compared with patients with no *CYP3A4*22* genotype. *CYP2C19*2* and *CYP2B6*6* alleles showed only a slight impact on ENDO.

Use of weak/moderate and potent CYP2D6 inhibitors decreased median ENDO $C_{ss,trough}$ in NM patients by 23% (from 37 to 28 nM) and 47% (to 19 nM), respectively, whereas in UM patients the median ENDO $C_{ss,trough}$ were decreased by 27% (from 46 to 34 nM) and 48% (to 24 nM), respectively.

The dose-adjustment simulations were performed for PM and IM patients (*CYP3A4*22*, *CYP2C19*2*, and *CYP2B6*6* noncarriers, 48 years old and 64 kg) and the results are presented in **Figure 4**. A dose increase from 20 to 40 mg/day in IM patients increased the number of patients reaching the ENDO target of 16 nM from 74% to 97%, respectively (**Figure 4a**). Concerning CYP2D6 PM patients, a dose increase from 20 to 40, 60, and 80 mg/day increased the number of patients reaching the ENDO target of 16 nM from 14% to 54%, 81%, and 92%, respectively. The evaluation of AAS following dose adjustment is presented in **Figure 4b**. A higher number of PM and IM patients reached the previously proposed AAS target threshold of 1,798 following a dose adjustment, compared with when ENDO $C_{ss,trough}$ is considered. Indeed, a dose of 60 mg/day in PM patients and 40 mg/day in IM patients resulted in 99% of the patients reaching the AAS target. The same trends were observed using the reference value of the median ENDO concentration or AAS, as presented in **Figure 4a,b**.

Although the number of IM patients reaching 16 nM ENDO target at standard dose is 74%, the simulations performed with the model including CYP2D6 diplotype on $k_{NDT/ENDO}$ (**Figure S2**) show that this number is indeed lower for IM/PM and IM/IM (39% and 48%, respectively) than for NM/PM patients (84%), which are all classified as IM phenotype. Therefore, patients with IM/PM or IM/IM diplotype may require 40 mg/day whereas NM/PM would reach adequate ENDO or AAS levels with 20 mg/day.

DISCUSSION

In our study, the sparse steady-state PK data for TAM and 6 metabolites in 928 patients with adjuvant breast cancer were adequately described by a 7-compartment model. To our knowledge, this is the first PK model to simultaneously incorporate the data for TAM and six metabolites, allowing for a more accurate quantification of the impact of genetic covariates on the respective metabolic pathways. The model enabled us to quantify the impact of

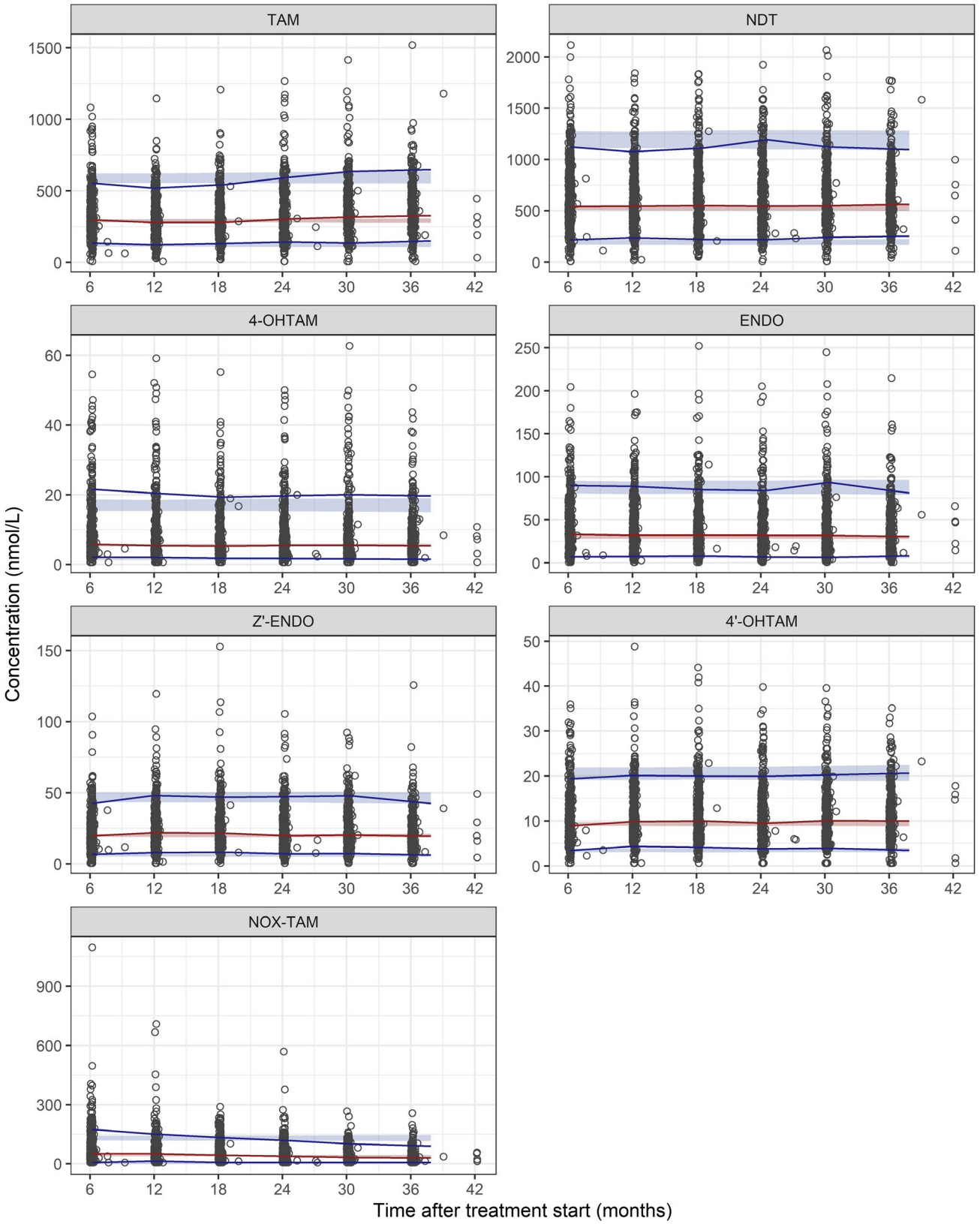

Figure 2 Visual predictive check for tamoxifen (TAM), N-desmethyltamoxifen (NDT), 4-hydroxytamoxifen (4-OHTAM), endoxifen (ENDO), Z′-endoxifen (Z′-ENDO), 4′-hydroxytamoxifen (4′-OHTAM), and tamoxifen N-oxide (NOX-TAM) based on 1,000 replicates of the original dataset using the final model. The shaded areas represent the 95% confidence intervals around the 5th, 50th (median), and 95th percentile of the simulated concentrations, the lines represent the 5th, 50th (median), and 95th percentile of the observed concentrations and the circles represent the observed concentrations. [Colour figure can be viewed at wileyonlinelibrary.com]

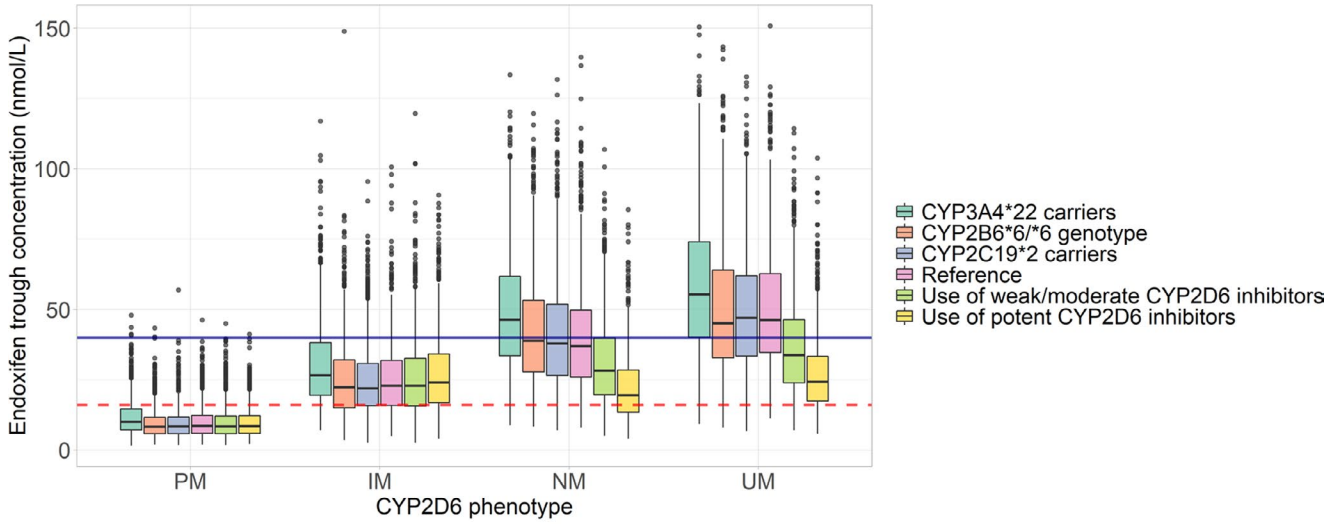

Above median in NM (%)	0.4	0.2	0.1	0.1	0.1	0.1	23	13	13	13	13	17	62	47	46	43	25	8.3	75	60	62	63	37	16
Above 16 nmol/L threshold (%)	19	9.2	10	13	13	11	85	71	74	75	74	77	98	96	96	95	86	65	99	97	98	99	92	79

Figure 3 Simulations of steady-state trough endoxifen concentrations according to CYP2D6 phenotype, *CYP3A4*22*, *CYP2C19*2*, and *CYP2B6*6* genotypes and use of CYP2D6 inhibitors using structural and interindividual parameter estimates from the final model (20 mg/day tamoxifen dose). For each combination, n = 1,000 endoxifen concentrations were simulated. The simulated subjects have a wild-type genotype for *CYP3A4*22*, *CYP2C19*2*, and *CYP2B6*6* and no use of concomitant CYP2D6 inhibitors (reference) unless otherwise specified. For simulations, median population values of body weight (64 kg) and age (48 years) were used. The solid line represents the median plasma ENDO steady-state concentration observed in patients with CYP2D6 NM phenotype, *CYP3A4*22*, *CYP2C19*2*, *CYP2B6*6* noncarriers and no concomitant intake of CYP2D6 inhibitors of 40 nM. The dashed line represents the previously proposed plasma endoxifen therapeutic threshold of 16 nM.[8] IM, intermediate metabolizer; NM, normal metabolizer; PM, poor metabolizer; UM, ultra-rapid metabolizer. [Colour figure can be viewed at wileyonlinelibrary.com]

CYP2D6 phenotype, *CYP3A4*22, CYP2C19*2*, and *CYP2B6*6* genotypes, the use of CYP2D6 weak/moderate and potent inhibitors, as well as age and BW, on TAM metabolism, and was subsequently used to perform dose-adjustment simulations.

The PK parameters for NOX-TAM, 4′-OHTAM and Z′-ENDO were estimated to range at very small values. However, the PKs of these metabolites has not been evaluated before, hence reference values were not available in the literature. Based on the mean estimates of V_{TAM}, $k_{TAM/NDT}$, $k_{TAM/4\text{-}OHTAM}$, $k_{TAM/4'\text{-}OHTAM}$, and $k_{TAM/NOX\text{-}TAM}$ in our model, the mean oral clearance of TAM was 7.2 L/hours, which is consistent with the previously reported value of 6.6 L/hours.[24] The developed model showed good predictive performance based on VPC and on comparative simulations with a recently published model and observed values.[16,22]

In the covariate analysis, CYP2D6 phenotype was significantly associated with NDT to ENDO and TAM to 4-OHTAM conversions. In particular, the mean $k_{NDT/ENDO}$ was decreased by 84% and 47% in PM and IM patients, respectively, and increased by 27% in UM patients, compared with NM patients.

An additional analysis was performed with CYP2D6 diplotype included on $k_{NDT/ENDO}$. NM/IM (AS = 1.25 or 1.5), NM/PM (AS = 1), IM/IM (AS = 0.5 or 1), IM/PM (AS = 0.25 or 0.5), and PM/PM (AS = 0) patients showed a decrease in $k_{NDT/ENDO}$ by 32%, 43%, 70%, 74%, and 85%, respectively, compared with NM/NM patients. Clinical Pharmacogenetics Implementation Consortium (CPIC) guidelines have recently updated the *CYP2D6* genotype to phenotype translation system and patients with an AS = 1 are now categorized as IM rather than NM, as was previously the case.[25] Our data show that the AS = 1 group is quite heterogeneous and IM/IM patients have a lower CYP2D6 activity than NM/PM patients, even though they have the same AS. IM/IM patients had an estimate of $k_{NDT/ENDO}$ close to IM/PM patients, therefore, assignment of IM phenotype seems appropriate for both these diplotypes. However, the estimate of $k_{NDT/ENDO}$ in NM/PM patients was closest to that in NM/IM patients, which supports the assignment of NM phenotype for NM/PM patients rather than IM phenotype.

An advantage of our analysis is the use of a PK model for estimation of the impact of CYP2D6 activity for each diplotype/phenotype on NDT to ENDO metabolic pathway, which has not been performed before. The use of $k_{NDT/ENDO}$ as a marker of CYP2D6 activity is justified by the fact that CYP2D6 is the only enzyme involved in this metabolic route. Inclusion of CYP2D6 phenotype on $k_{NDT/ENDO}$ explained 37% of the IIV, which is consistent with values found in previous studies (between 19% and 57%), evaluating the impact of CYP2D6 on the NDT/ENDO metabolic ratio.[26,27]

In our study, patients carrying *CYP3A4*22* allele (associated with a decreased mRNA expression and decreased enzyme activity[28]) had 23% and 19% lower $k_{TAM/NDT}$ and $k_{e,NDT}$, respectively. *CYP3A4*22* was previously associated with a decreased TAM/NDT metabolic ratio.[27] This is also consistent with

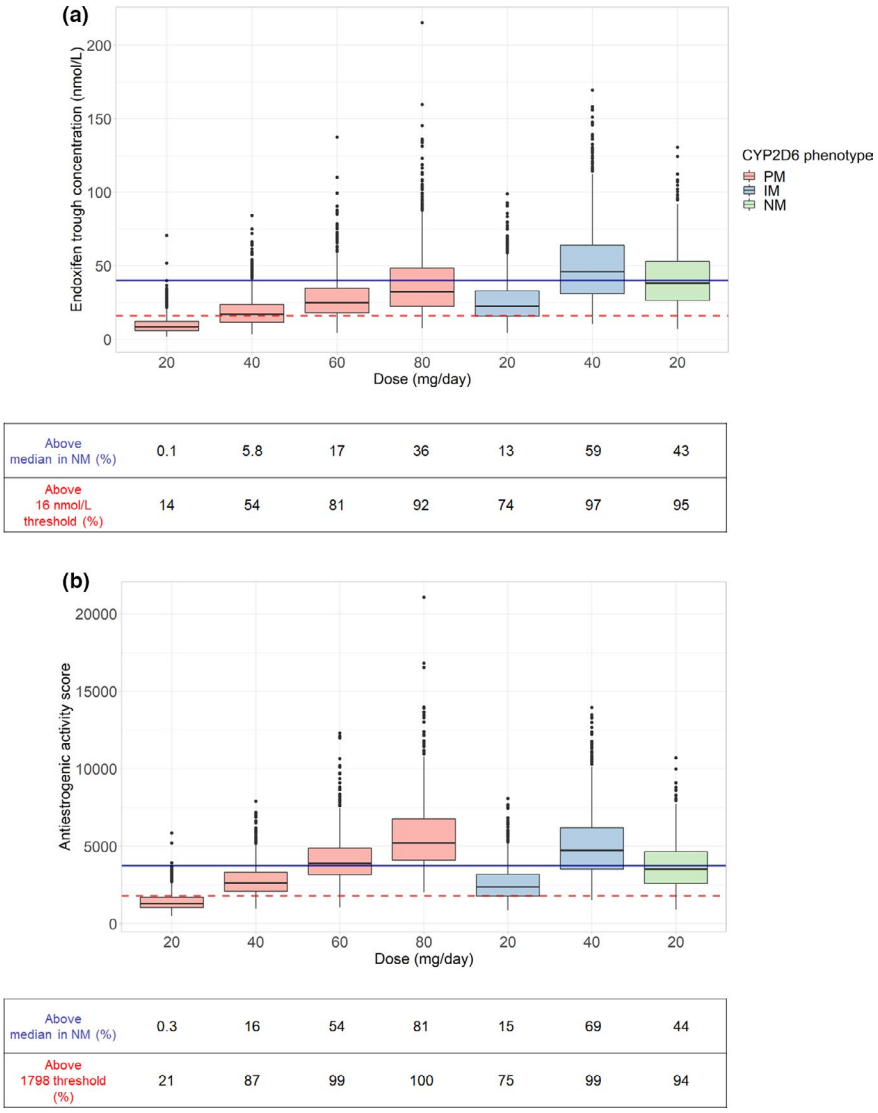

Figure 4 Simulations of alternative dosing regimens for patients with CYP2D6 PM and IM phenotype according to steady-state trough endoxifen concentrations or antiestrogenic activity score. Simulations (n = 1,000) were performed using structural and interindividual parameter estimates from the final model. The subjects all have a wild-type genotype for *CYP3A4*22*, *CYP2C19*2*, and *CYP2B6*6*, no use of concomitant CYP2D6 inhibitors and median population values of body weight (64 kg) and age (48 years). The solid line represents (**a**) the median plasma ENDO steady-state concentration of 40 nM and (**b**) the median antiestrogenic activity score of 3,753 observed in CYP2D6 NM phenotype, *CYP3A4*22*, *CYP2C19*2*, *CYP2B6*6* noncarriers, and no concomitant intake of CYP2D6 inhibitors. The dashed line represents the previously proposed efficacy thresholds for (**a**) plasma endoxifen concentration of 16 nM[8] and (**b**) antiestrogenic activity score of 1,798.[23]ENDO, endoxifen; IM, intermediate metabolizer; NM, normal metabolizer; PM, poor metabolizer. [Colour figure can be viewed at wileyonlinelibrary.com]

previous *in vitro* studies showing that CYP3A is involved in the metabolism of NDT into α-hydroxy-N-desmethyltamoxifen and N,N-didesmethyltamoxifen.[1]

In the current analysis, *CYP2C19*2* carriers showed a 13% decrease in $k_{TAM/4\text{-}OHTAM}$, which is consistent with the involvement of CYP2C19 in this metabolic pathway,[1] although the impact of *CYP2C19*2* on the formation of ENDO has not been clearly demonstrated in previous studies.[2,29] In addition to CYP2C19, it has been previously proposed that *CYP2C9* variant allele may alter formation of 4-OHTAM.[2] Unfortunately, *CYP2C9* was not genotyped in our study and its effect on $k_{TAM/4\text{-}OHTAM}$ could not be quantified, which probably accounts for part of the remaining IIV on $k_{TAM/4\text{-}OHTAM}$ after inclusion of significant covariates (50.6%).

In addition, patients carrying *CYP2B6*6/*6* genotype showed a mean decrease of 23% in $k_{TAM/NOX\text{-}TAM}$ compared with patients carrying *CYP2B6*1/*6* or *CYP2B6*1/*1*, consistent with decreased enzyme activity associated with **6* allele.[30] However, CYP2B6 is involved in the metabolism of TAM into 4-OHTAM and 4′-OHTAM[1,2] whereas the metabolism of TAM into NOX-TAM is mainly mediated by human flavin-containing monooxygenase 1 and flavin-containing monooxygenase 3.[31] Therefore, our result might reflect the impact of *CYP2B6*6* on the elimination of TAM.

In the covariate analysis, age was significantly associated with $k_{TAM/NDT}$, $k_{TAM/4\text{-}OHTAM}$, and $k_{NDT/ENDO}$ and $k_{TAM/NOX\text{-}TAM}$, leading to decreased ENDO concentrations in older patients. One explanation could be decreased enzymatic activity in older patients causing lower formation of ENDO. However, contradictory results concerning the impact of age on TAM PK have been reported with either no significant association found[32,33] or increased levels of TAM, NDT, and ENDO observed in older patients.[16,34–36] Only 5.6% of our patients were over 65 years old, which limits the interpretation of the age effect on ENDO.

A significant increase in $k_{e,NDT}$ with increasing BW was found, consistent with previous reports on decreased NDT and ENDO concentrations in patients with high BW.[8,9,16,33]

Evaluation of alternative dosing regimens through simulations showed that a dose increase from 20 to 40 mg/day in IM patients increased the number of patients reaching the ENDO target of 16 nM from 74% to 97%. Concerning CYP2D6 PM patients, a dose increase from 20 to 40, 60, and 80 mg/day increased the number of patients reaching the ENDO target of 16 nM from 14% to 54%, 81%, and 92%, respectively. On the basis of these results, a dose of 40 mg/day and 80 mg/day could be proposed in IM and PM patients, respectively. Similar findings were reported in dose-escalation studies performed in patients with IM and PM phenotypes or with ENDO concentrations below certain thresholds.[37,38]

Furthermore, our PK model can be used to simulate concentrations of active metabolites and calculate AAS, which can serve as a surrogate for clinical response, based on the hypothesis that other TAM metabolites apart from ENDO contribute to antitumoral activity. When we considered AAS, a higher number of IM and PM patients reached similar levels as NM patients following the dose adjustment compared with when ENDO $C_{ss,trough}$ was taken into account. In addition, a dose increase to 60 mg/day in PM patients could be sufficient, based on AAS. However, the clinical utility of AAS has only been described in one retrospective analysis[23] and future research should examine its use as a marker for TAM efficacy.

Interestingly, simulations performed on 15,000 virtual European female patients with early breast cancer using a physiologically-based pharmacokinetic model for TAM based on *in vitro* and *in vivo* data,[39] led to similar dose recommendations as in our model, confirming the robustness of our analysis.

The advantage of the present PK model is the possibility of *a priori* prediction of TAM dose necessary to achieve target ENDO levels. To date, the clinical utility of ENDO therapeutic drug monitoring remains uncertain as the therapeutic threshold of 16 nM associated with a better outcome[8] was not confirmed in the prospective CYPTAM study[11] nor in two other studies[40,41] carried out in patients with metastatic breast cancer. However, these latter results cannot be extrapolated to early breast cancer populations. Moreover, a recent study[42] showed that nonadherent patients have a higher risk for relapse, implying that underexposure to active metabolites could lead to a lack of efficacy.

Furthermore, the CPIC recommends increasing TAM dose to 40 mg/day in IM and PM patients for whom the alternative therapy by aromatase inhibitors cannot be prescribed.[25] The dose increment to 40 mg/day in patients with ENDO levels under 16 nM has already been implemented in some hospitals.[43] However, as shown by our simulations, a dose increase to 40 mg/day in PM patients is not sufficient to reach similar ENDO or AAS levels as those observed in NM patients. It should be noted that doses higher than 40 mg/day have not been approved in a clinical setting, although doses up to 120 mg/day have been administered to patients with adjuvant breast cancer for a limited period of 2 months in dose escalation studies.[38] Although no increase in toxicity was observed at higher doses, the longitudinal benefit/risk ratio of a chronic high dose exposition is not known.

In this study, adherence to treatment was recorded as declared number of doses taken in the month preceding the PK sampling. The proportion of patients considered as nonadherent (defined as < 80% of theoretical number of doses taken) represented only 1% of the total number of visits. Therefore, the adherence data were not included in the PK model. Nevertheless, a recent study showed that at least 50% of patients with undetectable or low TAM concentrations did not admit to nonadherence.[44] Therefore, the reported adherence in our study may have been underestimated; this will be evaluated in our future investigations.

CONCLUSION

The present study is the first to explore the PK of TAM and six of its metabolites using a population approach based on data from a large, prospective, longitudinal study. It provides important information on the quantitative contribution of genetic polymorphisms, comedications, and demographic characteristics to TAM metabolism and their impact on plasma ENDO levels, possibly the most important surrogate for clinical response. Evaluation of the relationship between TAM PK and adverse events based on data from the PHACS study is planned in the near future. Finally, the developed PK model could be used to individually adapt the dose based on CYP2D6 phenotype and ENDO plasma exposure if the clinical utility of PK-guided dosing for TAM is demonstrated.

SUPPORTING INFORMATION

Supplementary information accompanies this paper on the *Clinical Pharmacology & Therapeutics* website (www.cpt-journal.com).

FUNDING

The PHACS study (NCT01127295) was supported by a grant from the French Ministry of Health (PHRC 2009 #09-18-005). Alicja Puszkiel received a grant from French National Institute of Health and Medical Research (Inserm).

CONFLICT OF INTEREST

The authors declared no conflict of interests for this work.

AUTHOR CONTRIBUTIONS

A.P., F.T., and M.W.-K. wrote the manuscript. H.R., A.E., J.R., J.C.B., M.D., W.J., T.F., E.C., F.T., and M.W.-K. designed the research. A.P., C.A., C.V., A.E., V.L.M., J.C.B., J.R., C.D., F.D., M.D., L.V.-B., W.J., N.D., C.B.-M., H.L.-M., H.R., F.T., and M.W.-K. performed the research. A.P., C.A., A.E., V.L.M, J.C.B., J.R., T.F., E.C., F.T., and M.W.-K. analyzed the data.

1. Desta, Z., Ward, B.A., Soukhova, N.V. & Flockhart, D.A. Comprehensive evaluation of tamoxifen sequential biotransformation by the human cytochrome P450 system in vitro:

prominent roles for CYP3A and CYP2D6. *J. Pharmacol. Exp. Ther.* **310**, 1062–1075 (2004).
2. Mürdter, T.E. *et al*. Activity levels of tamoxifen metabolites at the estrogen receptor and the impact of genetic polymorphisms of phase I and II enzymes on their concentration levels in plasma. *Clin. Pharmacol. Ther.* **89**, 708–717 (2011).
3. Jordan, V.C. & Chem, C. Metabolites of tamoxifen in animals and man: Identification, pharmacology, and significance. *Breast Cancer Res. Treat.* **2**, 123–138 (1982).
4. Lim, Y.C., Desta, Z., Flockhart, D.A. & Skaar, T.C. Endoxifen (4-hydroxy-N-desmethyl-tamoxifen) has anti-estrogenic effects in breast cancer cells with potency similar to 4-hydroxy-tamoxifen. *Cancer Chemother. Pharmacol.* **55**, 471–478 (2005).
5. Goetz, M.P. *et al*. The impact of cytochrome P450 2D6 metabolism in women receiving adjuvant tamoxifen. *Breast Cancer Res. Treat.* **101**, 113–121 (2007).
6. Rae, J.M. *et al*. CYP2D6 and UGT2B7 genotype and risk of recurrence in tamoxifen-treated breast cancer patients. *J. Natl. Cancer Inst.* **104**, 452–460 (2012).
7. Regan, M.M. *et al*. CYP2D6 genotype and tamoxifen response in postmenopausal women with endocrine-responsive breast cancer: the Breast International Group 1–98 Trial. *J. Natl. Cancer Inst.* **104**, 441–451 (2012).
8. Madlensky, L. *et al*. Tamoxifen metabolite concentrations, CYP2D6 genotype, and breast cancer outcomes. *Clin. Pharmacol. Ther.* **89**, 718–725 (2011).
9. Saladores, P. *et al*. Tamoxifen metabolism predicts drug concentrations and outcome in premenopausal patients with early breast cancer. *Pharmacogenomics J.* **15**, 84–94 (2015).
10. Helland, T. *et al*. Serum concentrations of active tamoxifen metabolites predict long-term survival in adjuvantly treated breast cancer patients. *Breast Cancer Res.* **19**, 125 (2017).
11. Sanchez-Spitman, A. *et al*. Tamoxifen pharmacogenetics and metabolism: results from the prospective CYPTAM study. *J. Clin. Oncol.* **37**, 636–646 (2019).
12. Sanchez-Spitman, A.B. *et al*. Exposure–response analysis of endoxifen serum concentrations in early-breast cancer. *Cancer Chemother. Pharmacol.* **85**, 1141–1152 (2020).
13. Goetz, M.P. *et al*. Tamoxifen metabolism and breast cancer recurrence: a question unanswered by CYPTAM. *J. Clin. Oncol.* **37**, 1982–1983 (2019).
14. Brauch, H., Schroth, W., Mürdter, T. & Schwab, M. Tamoxifen pharmacogenetics and metabolism: the same is not the same. *J. Clin. Oncol.* **37**, 1981–1982 (2019).
15. ter Heine, R. *et al*. Population pharmacokinetic modelling to assess the impact of CYP2D6 and CYP3A metabolic phenotypes on the pharmacokinetics of tamoxifen and endoxifen. *Br. J. Clin. Pharmacol.* **78**, 572–586 (2014).
16. Mueller-Schoell, A. *et al*. Obesity alters endoxifen plasma levels in young breast cancer patients: a pharmacometric simulation approach. *Clin. Pharmacol. Ther.* **108**, 661–670 (2020).
17. Dahmane, E. *et al*. Population pharmacokinetics of tamoxifen and three of its metabolites in breast cancer patients. 22nd PAGE (Population Approach Group Europe) conference, 11-14 June 2013, Glasgow, Scotland, UK. https://www.page-meeting.org/default.asp?abstract=2910 (2013).
18. Puszkiel, A. *et al*. Factors affecting tamoxifen metabolism in patients with breast cancer: preliminary results of the French PHACS study. *Clin. Pharmacol. Ther.* **106**, 585–595 (2019).
19. Arellano, C., Allal, B., Goubaa, A., Roché, H. & Chatelut, E. An UPLC–MS/MS method for separation and accurate quantification of tamoxifen and its metabolites isomers. *J. Pharm. Biomed. Anal.* **100**, 254–261 (2014).
20. Caudle, K.E. *et al*. Standardizing CYP2D6 genotype to phenotype translation: consensus recommendations from the clinical pharmacogenetics implementation consortium and Dutch Pharmacogenetics Working Group. *Clin. Transl. Sci.* **13**, 116–124 (2020).
21. Courlet, P. *et al*. Influence of drug-drug interactions on the pharmacokinetics of atorvastatin and its major active metabolite ortho-OH-atorvastatin in aging people living with HIV. *Clin. Pharmacokinet.* **59**, 1037–1048 (2020).
22. Teft, W.A. *et al*. CYP3A4 and seasonal variation in vitamin D status in addition to CYP2D6 contribute to therapeutic endoxifen level during tamoxifen therapy. *Breast Cancer Res. Treat.* **139**, 95–105 (2013).
23. de Vries Schultink, A.H.M. *et al*. An Antiestrogenic Activity Score for tamoxifen and its metabolites is associated with breast cancer outcome. *Breast Cancer Res. Treat.* **161**, 567–574 (2017).
24. Hutson, P.R., Love, R.R., Havighurst, T.C., Rogers, E. & Cleary, J.F. Effect of exemestane on tamoxifen pharmacokinetics in postmenopausal women treated for breast cancer. *Clin. Cancer Res.* **11**, 8722–8727 (2005).
25. Goetz, M.P. *et al*. Clinical Pharmacogenetics Implementation Consortium (CPIC) guideline for CYP2D6 and tamoxifen therapy. *Clin. Pharmacol. Ther.* **103**, 770–777 (2018).
26. Hertz, D.L. *et al*. In vivo assessment of the metabolic activity of CYP2D6 diplotypes and alleles. *Br. J. Clin. Pharmacol.* **80**, 1122–1130 (2015).
27. Sanchez Spitman, A.B. *et al*. Effect of CYP3A4*22, CYP3A5*3, and CYP3A combined genotypes on tamoxifen metabolism. *Eur. J. Clin. Pharmacol.* **73**, 1589–1598 (2017).
28. Wang, D., Guo, Y., Wrighton, S.A., Cooke, G.E. & Sadee, W. Intronic polymorphism in CYP3A4 affects hepatic expression and response to statin drugs. *Pharmacogenomics J.* **11**, 274–286 (2011).
29. Lim, J.S.L. *et al*. Association of CYP2C19*2 and associated haplotypes with lower norendoxifen concentrations in tamoxifen-treated Asian breast cancer patients. *Br. J. Clin. Pharmacol.* **81**, 1142–1152 (2016).
30. Zanger, U.M. & Klein, K. Pharmacogenetics of cytochrome P450 2B6 (CYP2B6): advances on polymorphisms, mechanisms, and clinical relevance. *Front. Genet.* **4**, 24 (2013).
31. Parte, P., Kupfer, D. & Pape, C.W. Oxidation of tamoxifen by human flavin-containing monooxygenase (FMO) 1 and FMO3 to tamoxifen-N-oxide and its novel reduction back to tamoxifen by human cytochromes P450 and hemoglobin. *Drug Metab. Dispos.* **33**, 1446–1452 (2005).
32. Schroth, W. *et al*. Improved prediction of endoxifen metabolism by CYP2D6 genotype in breast cancer patients treated with tamoxifen. *Front. Pharmacol.* **8**, 582 (2017).
33. Marcath, L.A. *et al*. Comprehensive assessment of cytochromes P450 and transporter genetics with endoxifen concentration during tamoxifen treatment. *Pharmacogenet. Genomics* **27**, 402–409 (2017).
34. Peyrade, F. *et al*. Age-related difference in tamoxifen disposition. *Clin. Pharmacol. Ther.* **59**, 401–410 (1996).
35. Lien, E.A. *et al*. Serum concentrations of tamoxifen and its metabolites increase with age during steady-state treatment. *Breast Cancer Res. Treat.* **141**, 243 (2013).
36. Klopp-Schulze, L. *et al*. Integrated data analysis of six clinical studies points toward model-informed precision dosing of tamoxifen. *Front. Pharmacol.* **11**, 283 (2020).
37. Irvin, W.J. *et al*. Genotype-guided tamoxifen dosing increases active metabolite exposure in women with reduced CYP2D6 metabolism: a multicenter study. *J. Clin. Oncol.* **29**, 3232–3239 (2011).
38. Dezentjé, V.O. *et al*. CYP2D6 genotype- and endoxifen-guided tamoxifen dose escalation increases endoxifen serum concentrations without increasing side effects. *Breast Cancer Res. Treat.* **153**, 583–590 (2015).
39. Dickschen, K. *et al*. Concomitant use of tamoxifen and endoxifen in postmenopausal early breast cancer: prediction of plasma levels by physiologically-based pharmacokinetic modeling. *Springerplus* **3**, 1–9 (2014).
40. Neven, P. *et al*. Tamoxifen metabolism and efficacy in breast cancer: a prospective multicenter trial. *Clin. Cancer Res.* **24**, 2312–2318 (2018).
41. Tamura, K. *et al*. CYP2D6 genotype-guided tamoxifen dosing in hormone receptor-positive metastatic breast cancer (TARGET-1): a randomized, open-label. Phase II study. *J. Clin. Oncol.* **38**, 558–566 (2020).

42. Pistilli, B. *et al*. Serum detection of nonadherence to adjuvant tamoxifen and breast cancer recurrence risk. *J. Clin. Oncol.* **38**, 2762–2772 (2020).
43. de Vries Schultink, A.H.M., Huitema, A.D.R. & Beijnen, J.H. Therapeutic drug monitoring of endoxifen as an alternative for CYP2D6 genotyping in individualizing tamoxifen therapy. *Breast J.* **42**, 38–40 (2018).
44. Pistilli, B. *et al*. Serum assessment of non-adherence to adjuvant endocrine therapy (ET) among premenopausal patients in the prospective multicenter CANTO cohort. *Ann. Oncol.* **29**, viii704 (2018).